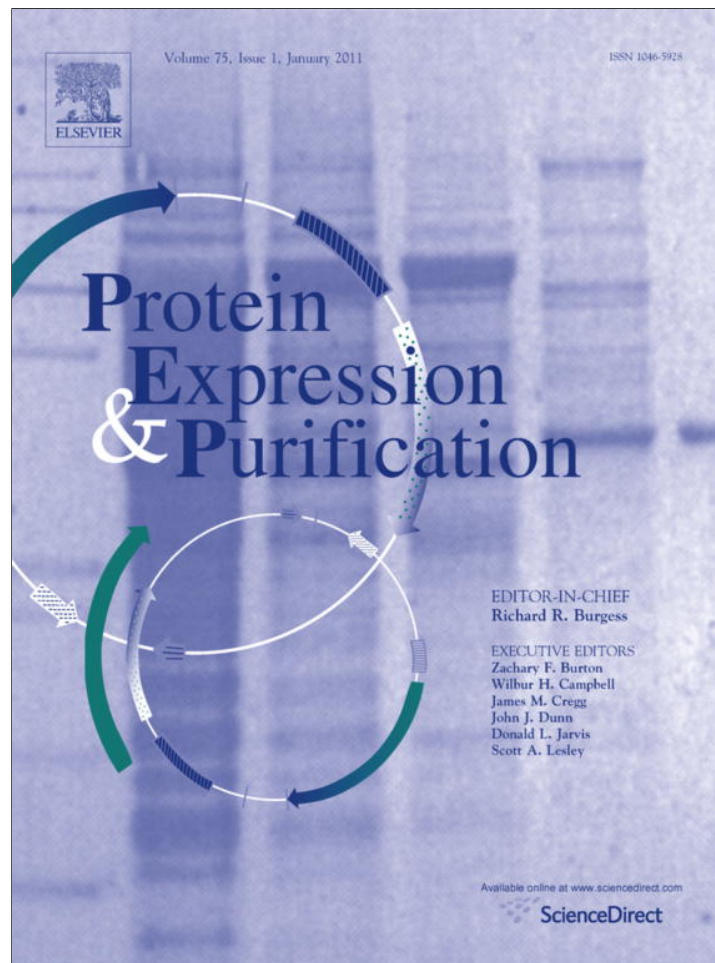


Provided for non-commercial research and education use.
Not for reproduction, distribution or commercial use.



(This is a sample cover image for this issue. The actual cover is not yet available at this time.)

This article appeared in a journal published by Elsevier. The attached copy is furnished to the author for internal non-commercial research and education use, including for instruction at the authors institution and sharing with colleagues.

Other uses, including reproduction and distribution, or selling or licensing copies, or posting to personal, institutional or third party websites are prohibited.

In most cases authors are permitted to post their version of the article (e.g. in Word or Tex form) to their personal website or institutional repository. Authors requiring further information regarding Elsevier's archiving and manuscript policies are encouraged to visit:

<http://www.elsevier.com/copyright>



Contents lists available at SciVerse ScienceDirect

Protein Expression and Purification

journal homepage: www.elsevier.com/locate/yprep

Efficient and versatile one-step affinity purification of *in vivo* biotinylated proteins: Expression, characterization and structure analysis of recombinant human glutamate carboxypeptidase II

J. Tykvarť ^{a,b}, P. Šácha ^{a,b}, C. Bařinka ^c, T. Knedlík ^{a,b}, J. Starková ^a, J. Lubkowski ^d, J. Konvalinka ^{a,b,*}

^a Gilead Sciences and IOCB Research Centre, Institute of Organic Chemistry and Biochemistry, Academy of Sciences of the Czech Republic, Flemingovo n. 2, Prague 6, Czech Republic

^b Department of Biochemistry, Faculty of Natural Science, Charles University, Albertov 6, Prague 2, Czech Republic

^c Institute of Biotechnology, Academy of Sciences of the Czech Republic, Videnska 1083, Prague 4, Czech Republic

^d Center for Cancer Research, National Cancer Institute at Frederick, Frederick, MD, USA

ARTICLE INFO

Article history:

Received 6 September 2011
and in revised form 28 November 2011
Available online 8 December 2011

Keywords:

Affinity purification
Biotin acceptor peptide
Recombinant protein expression
Biotin-protein ligase (BirA)
Co-localization
PSMA

ABSTRACT

Affinity purification is a useful approach for purification of recombinant proteins. Eukaryotic expression systems have become more frequently used at the expense of prokaryotic systems since they afford recombinant eukaryotic proteins with post-translational modifications similar or identical to the native ones.

Here, we present a one-step affinity purification set-up suitable for the purification of secreted proteins. The set-up is based on the interaction between biotin and mutated streptavidin. *Drosophila* Schneider 2 cells are chosen as the expression host, and a biotin acceptor peptide is used as an affinity tag. This tag is biotinylated by *Escherichia coli* biotin-protein ligase *in vivo*. We determined that localization of the ligase within the ER led to the most effective *in vivo* biotinylation of the secreted proteins. We optimized a protocol for large-scale expression and purification of AviTEV-tagged recombinant human glutamate carboxypeptidase II (Avi-GCP II) with milligram yields per liter of culture. We also determined the 3D structure of Avi-GCP II by X-ray crystallography and compared the enzymatic characteristics of the protein to those of its non-tagged variant. These experiments confirmed that AviTEV tag does not affect the biophysical properties of its fused partner.

Purification approach, developed here, provides not only a sufficient amount of highly homogenous protein but also specifically and effectively biotinylates a target protein and thus enables its subsequent visualization or immobilization.

© 2011 Elsevier Inc. All rights reserved.

Introduction

Purification of recombinant proteins via diverse affinity tags has recently largely replaced approaches utilizing the biophysical features of the proteins. Affinity tags based on the well-characterized biotin-avidin interaction (or its analogs) were among the first candidates for this application since this interaction is the strongest ($K_D \sim 10^{-15}$ M) non-covalent bond known in biology [1].

Ironically, the strength of the binding is a major drawback for its use as a purification technique, since the elution conditions would have to be so harsh that they would lead to destruction of the purified protein. One possible way to overcome this problem is to use site-directed mutagenesis to modify the streptavidin

molecule to have a K_D for biotin in the micromolar range, which is more suitable for purification purposes [2,3].

Enzymatic biotinylation of target proteins by biotin-protein ligase from *Escherichia coli* (BirA; EC 6.3.4.15) is often used instead of the less specific *in vitro* chemical biotinylation of free amino groups. In *E. coli*, this ligase recognizes and biotinylates the ϵ -amino group of a specific lysine residue within the biotin carboxyl carrier protein subunit of acetyl-CoA carboxylase [4,5]. Using combinatorial peptide libraries, a 15 amino acid peptide with one lysine residue specifically biotinylated by BirA was identified. The sequence was referred to as biotin acceptor peptide (BAP) or, more frequently, AviTag and it bears little similarity to the natural BirA substrate [6,7].

The biotinylation via BirA can proceed either *in vitro* or *in vivo*. The *in vivo* biotinylation, being a part of intracellular, post-translational modification of target proteins represents an elegant, high-yield approach [8–10]. AviTag is specifically recognized only by the BirA, therefore if other expression systems than *E. coli* are used for production of biotinylated proteins, the expressing cells

* Corresponding author. Address: Institute of Organic Chemistry and Biochemistry, ASCR, v.v.i. Flemingovo n. 2, 166 10 Prague 6, Czech Republic. Fax: +420 220 183 578.

E-mail address: jan.konvalinka@uochb.cas.cz (J. Konvalinka).

have to be co-transfected with plasmids coding for both targeted protein and *BirA*. Proteins biotinylated *in vivo* were successfully expressed in both mammalian [8,10–13] and insect [9,14,15] expression systems. In some of these studies, different cellular localizations of *BirA* (in cytoplasm, within the ER, or in the secretory pathway) were investigated showing a strong dependency of *BirA* localization on its biotinylation efficiency. In all these experiments, the biotinylated proteins were expressed as secreted proteins [10,11,15].

Besides the AviTag/*BirA*/mutated streptavidin system, there are other affinity purification approaches utilizing avidin or its analogs. Above all, the Strep-tag II/Strep-Tactin system is commonly used [16,17]. This system does not require additional transfection with *BirA* since the Strep-tag II binds directly to the Strep-Tactin molecule. On the other hand, the Strep-tag II affinity to Strep-Tactin is in the micromolar range, which is suitable for purification but might represent a drawback during visualization, immobilization, or specific uptake of a target protein. Generally, purification approaches based on the avidin–biotin interaction are very specific, ensuring a high homogeneity of the purified proteins. Achieving such a homogeneity may be an occasional problem with the use of other affinity tags, e.g. His-tag [18].

In this paper, we present an optimized one-step protocol for affinity purification of recombinant proteins expressed via the secretory pathway in insect cells with *BirA* localized within the ER. The purified protein, the extracellular portion of glutamate carboxypeptidase II (rhGCPII, amino acids 44–750)¹, is a 90 kD N-glycosylated metalloprotease [19,20]. GCPII (EC 3.4.17.21) belongs to the family of type II transmembrane proteins and is an interesting pharmaceutical target for prostate cancer imaging and treatment [21–23]. It is also implicated in neuropathological disorders [24] and has an unknown function in angiogenesis [25,26].

Materials and methods

Preparation of expression plasmid for N-terminally AviTEV-tagged proteins

DNA encoding the AviTEV tag was prepared *de novo* from six individual oligonucleotides with complementary overlaps. Short 5' overhangs were filled in with Phusion polymerase (Finnzymes). The following primers were used: Avi0-F (5'-aaaatgatcagggcctgaacgacatc-3'), Avi1-R (5'-atcttctgggcctcgaagatgctcttcaggcc-3'), Avi2-F (5'-ttcagggcccagaagatcgagtgccacg-3'), Avi3-R (5'-ggttctcgtccgctg ccgctgccctcgtgccactc-3'), Uni3-F (5'-gcagggcagcgagaacctgtact tccagggcagatctgaattcaaaaa-3'), and Uni4-R (5'-ttttgtaattcagatctg c-3'). Sequences encoding AviTag™ (Avidity) are underlined, and sequences encoding the TEV cleavage site are in bold. Two restriction sites introduced into the DNA are shown in italics, *BclI* at the 5' end and *BglII* at the 3' end of the sequence.

A standard PCR reaction was performed with a mixture of all primers. The resulting DNA construct was cleaved by *BclI* and *BglII* and inserted into the pMNAEXST, pre-cleaved with *BglII*, to create a plasmid for expression of N-terminally AviTEV-tagged rhGCPII. Both correct orientation and sequence of the prepared plasmid

were verified by sequencing. The resulting plasmid was denoted pMT/BiP/AviTEV/rhGCPII and contained AviTEV tag immediately downstream of the BiP peptide signal sequence for secretion. Additionally, the DNA encoding rhGCPII can be easily excised with *BglII* and *XhoI/XbaI* restriction enzymes, and DNA encoding a different secreted protein can be substituted.

Preparation of plasmids encoding differently localized *BirA*

The commercially available plasmid pBirAcm (Avidity) was used as a template for PCR reactions. To obtain a plasmid encoding cytoplasmic *BirA*, primers BirAKpnI-F (5'-atcgggtaccatgaaggataacaccgtgcc-3') and BirAnoKDELXhoI-R (5'-tctagactcgagtattctgcac tacgcagg-3') were used (restriction sites are italicized). The DNA amplicon was cleaved with *KpnI* and *XhoI* and ligated into the vector pMT/V5-HisA (Invitrogen). The resulting plasmid was denoted pMT/BirA. To obtain DNA encoding *BirA* retained within the endoplasmic reticulum (ER), primers BirABgIII-F (5'-ctcgggagatc tatgaaggataacaccgtgcc-3') and BirAXhoI-R (5'-tctagactcgagtta cgtcatcttttctgcactacgcagg-3') were used to amplify DNA from pBirAcm. The DNA was cleaved with *BglII* and *XhoI* and ligated into the vector pMT/BiP/V5-HisA (Invitrogen). The resulting plasmid was named pMT/BiP/BirA/KDEL. A plasmid encoding secreted *BirA* was obtained similarly, but primer BirAXhoI-R was substituted with BirAnoKDELXhoI-R. The resulting plasmid encoding secreted *BirA* was denoted pMT/BiP/BirA.

The correct sequences of all three plasmids were subsequently verified by sequencing.

Preparation of stable *Drosophila* S2 cell lines expressing Avi-GCPII and *BirA*

Drosophila S2 cells were transfected consecutively, first with 9 µg of pMT/BiP/AviTEV/rhGCPII together with 0.5 µg of pCoBlast (Invitrogen) and selected with the appropriate antibiotic. Afterwards, they were transfected with 9 µg of one of the three different plasmids encoding differently localized *BirA* together with 0.5 µg of pCoHygro (Invitrogen), as previously published [27]. The transfected cells were selected by cultivation with both Blastidicin (5 µg/mL, Invitrogen) and Hygromycin B (300 µg/mL, Invitrogen) until they regained growth. Two transfections were performed in case of *BirA* localized within ER to prepared two individual polyclonal stable cell lines of S2 cells.

The 2.10⁶ cells of each stable transfectant were transferred to 35 mm Petri dish supplemented with 2 mL SF900II medium (Invitrogen). The protein expression was induced next day by 1 mM CuSO₄ (Sigma). Three days post-induction, the cells were harvested by centrifugation, and the medium was analyzed by Western blot.

Large-scale expression of Avi-GCPII and rhGCPII in *Drosophila* S2 cells

The protocol for large-scale expression of Avi-GCPII was almost identical to that previously described [19]. The only modification was the final volume of the cell suspension, which changed from 0.5 to 1 L. Different volumes of cell culture supplements were used accordingly. The protocol for large-scale expression and purification of rhGCPII was identical to that described previously [19].

Purification of Avi-GCPII on Streptavidin Mutein Matrix

The commercial protocol for Streptavidin Mutein Matrix™ (Roche) was used as a starting point for optimization of the purification protocol. Phosphate buffer was replaced with Tris-HCl buffer, since phosphate acts as a weak inhibitor of GCPII [28]. Additional optimization experiments were performed on a small-scale with 9 mL of conditioned medium and 200 µL of mutein resin

¹ Abbreviations used: GCPII, glutamate carboxypeptidase II; rhGCPII, extracellular portion of GCPII consisting of amino acids 44–750; Avi-GCPII, molecule of rhGCPII fused at its N-terminus with AviTEV tag; TEV protease, tobacco etch virus protease; Ac-Asp-Glu, N-acetyl-L-aspartyl-L-glutamate; Ac-Asp-Met, N-acetyl-L-aspartyl-L-methionine; 2-PMPA, 2-(phosphonomethyl)-pentanedioic acid; BAP, biotin acceptor peptide; BirA, biotin-protein ligase from *Escherichia coli*; ER, endoplasmic reticulum; SDS-PAGE, sodium dodecyl sulfate-polyacrylamide gel electrophoresis; FBS, fetal bovine serum; PBS, phosphate buffered saline; TBS, tris buffered saline; Tris, tris(hydroxymethyl)aminomethane; HPLC, high-performance liquid chromatography; HRP, horseradish peroxidase; Neu, NeutrAvidin; S2 cells, Schneider 2 cells; r.m.s.d, root mean square deviation.

(i.e. 400 μ L of resin mixture with 20% ethanol). Following optimization, large-scale purification of Avi-GCPII was performed.

Conditioned medium from S2 cells (0.8 L) was centrifuged at 3400g for 30 min and then concentrated to 70 mL at 4 °C using a LabScale™ TFF system (Millipore) with a Pellicon XL Biomax50 cassette (Millipore). All subsequent purification steps were performed at 4 °C. The concentrated medium was mixed with equilibration buffer (450 mM NaCl, 300 mM Tris-HCl, pH 7.2) in a 2:1 ratio (fraction L). Equilibrated medium was mixed with 1.6 mL of murein resin, which had been washed several times with washing buffer (150 mM NaCl, 100 mM Tris-HCl, pH 7.2), and incubated overnight on a rocker. The next day, a disposable gravity column (Thermo Scientific) was used to separate the resin from the equilibrated medium (fraction FT). The murein resin was washed with 30 mL of washing buffer and then 1.6 mL of elution buffer (150 mM NaCl, 2 mM D-biotin, 100 mM Tris-HCl, pH 7.2) was applied to the column to replace the remaining wash buffer (fraction W). The column was sealed and the resin was incubated with elution buffer for 1 h. Then, the bound Avi-GCPII protein was eluted with 7 mL of elution buffer to obtain seven 1 mL elution fractions (fractions E1–7). Following the purification procedure, the Streptavidin Murein Matrix™ was regenerated and stored according to the manufacturer's protocol.

After the first purification and regeneration, the flow-through fraction and regenerated resin were mixed again and the whole purification procedure was repeated. All fractions were analyzed by reducing SDS-PAGE. The E1 and E2 fractions were dialyzed against appropriate buffer overnight, aliquoted and stored at –80 °C until further use.

SDS-PAGE and Western blotting

Protein samples were resolved by reducing, 0.1% sodium dodecyl sulfate (SDS), polyacrylamide gel electrophoresis (PAGE). Following SDS-PAGE, gels were either stained using Coomassie Brilliant Blue R-250 (Thermo Scientific), silver-stained, or electroblotted. For N-terminal sequencing, the proteins were transferred onto a polyvinylidene difluoride (PVDF) membrane, which was stained with Coomassie Brilliant Blue G-250 (Thermo Scientific).

Proteins were transferred onto a nitrocellulose membrane for detection by a specific antibody against rhGCPII (GCP-04) or NeuHRP (Thermo Scientific). The membrane was blocked with Blocker™ Casein in TBS (Thermo Scientific) for 1 h. For detection of rhGCPII, GCP-04 (1 mg/mL) was diluted 1:5000 in casein blocker, incubated overnight, washed several times with 0.05% Tween 20 in PBS, and incubated for 1 h with HRP-conjugated goat anti-mouse antibody (1 mg/mL; Thermo Scientific) diluted in casein blocker in a 1:25000 ratio. For detection of biotinylated proteins, NeuHRP (1 mg/mL) was diluted 1:2500 in casein blocker and incubated with the membrane for 1 h.

Afterwards, the membranes were washed with 0.05% Tween 20 in PBS several times to remove either Neu-HRP or HRP-conjugated goat anti-mouse antibody. The blots were developed using Super-Signal West Dura Chemiluminescence Substrate (Thermo Scientific) according to the manufacturer's protocol. Reactive bands were visualized on a LAS-3000 CCD camera (FujiFilm). If necessary, densitometry analysis was performed using ImageJ software v1.43 [29].

Cleavage of AviTEV tag from Avi-GCPII by TEV protease

Purified Avi-GCPII was diluted to a final concentration of 1 μ g/mL and mixed with His-TEV(S219 V)-Arg protease in an equimolar ratio or with a 100-fold molar excess of TEV protease. Equivalent reference mixture, without TEV protease, was also prepared. Five microliters of concentrated TBS buffer (1.5 M NaCl, 0.5 M Tris-HCl, pH 7.6) was added to each reaction, and the final volume

was adjusted to 50 μ L with distilled water. Mixtures were incubated overnight at 4 °C and analyzed on Western blots. Similar experiments were performed under identical conditions substituting concentrated TBS buffer with concentrated TEV buffer (10 mM β -mercaptoethanol, 5 mM EDTA, 0.5 M Tris-HCl, pH 8.0) or concentrated MOPS buffer (0.2 M NaCl, 0.2 M MOPS, pH 7.4).

Inhibition of Avi-GCPII degradation

Twenty microliters of purified Avi-GCPII (40 μ g/mL) was mixed with 5 μ L of inhibitor or water (negative control) to achieve a final concentration of 200 μ M for EDTA (Sigma-Aldrich), 2-PMPA, Pefabloc SC (Roche) and E-64 (Sigma-Aldrich) or 2 μ M for Pepstatin A (Sigma-Aldrich). Reactions were incubated at room temperature and 6 μ L samples were taken sequentially every other day and analyzed by SDS-PAGE.

Crystallization and data collection

The Avi-GCPII stock solution (10 mg/mL) was mixed with 1/10 volume of 1 mM 2-PMPA inhibitor, and the crystallization droplets were prepared by combining 2 μ L of the complex solution with 2 μ L of the reservoir solution containing 33% pentaerythritol propoxylate (Hampton Research), 1% polyethylene glycol 3350 (Fluka), and 100 mM Tris-HCl, pH 8.0. Crystals were grown by the hanging drop vapor diffusion method at 293 K.

Crystals were flash-frozen in liquid nitrogen directly from the reservoir solution, and the diffraction data were collected at 100 K using synchrotron radiation at the Southeast Regional Collaborative Access Team sector 22 beamlines BM of the Advanced Photon Source (Argonne, IL, USA) at an X-ray wavelength of 1.0 Å. The complete dataset was collected from a single crystal using the MarMosaic 225 mm CCD detector. Data processing was performed with the HKL2000 software package [30].

Structure determination and refinement

Since the crystal of the Avi-GCPII/2-PMPA complex was isomorphous with the crystals of rhGCPII containing the same inhibitor (PDB entry 2PVW) [31], the latter (without the inhibitor and water molecules) was used as the starting model for the structural refinement based on the X-ray data collected from a crystals of the Avi-GCPII/2-PMPA complex. Calculations were performed with the program Refmac 5.1 [32], and the refinement protocol was interspersed with manual corrections to the model using Coot [33]. The stereochemical quality of the final model was evaluated using MolProbity [34] and the final model, together with experimental amplitudes, deposited in the RCSB Protein Data Bank (entry code 3RBU). During the refinement process, 1363 of the randomly selected reflections were kept aside for cross-validation (Rfree).

Radioenzymatic assay of carboxypeptidase activity

To determine the kinetic constants of Ac-Asp-Glu cleavage, radioenzymatic assays using [³H]-Ac-Asp-Glu (radiolabelled on the terminal glutamate; 50 Ci/mmol in Tris buffer, Perkin-Elmer) were performed as previously described [27,28] with several modifications.

Briefly, appropriate amount of enzyme solution in reaction buffer (20 mM NaCl, 20 mM MOPS, pH 7.4) was pre-incubated for 10 min at 37 °C in a final volume of 90 μ L. The reaction was started by addition of a 10 μ L mixture of unlabeled and radioactive Ac-Asp-Glu with different overall concentration ranging from 200 nM to 50 μ M (containing 50 nM ³H-Ac-Asp-Glu together with corresponding amount of unlabeled Ac-Asp-Glu) and 100 μ M

to 400 μM (containing 100 nM ^3H -Ac-Asp-Glu together with corresponding amount of unlabeled Ac-Asp-Glu). Reactions were then incubated at 37 °C and after 20 min were stopped with 100 μL of ice-cold stopping solution (2 mM β -mercaptoethanol, 200 mM sodium phosphate, pH 7.4). Free glutamate was separated from the uncleaved substrate by ion exchange chromatography, and quantified by liquid scintillation using the Rotiszint ECO Plus scintillation cocktail (Roth) and Tri-Carb 2900TR liquid scintillation counter (Perkin–Elmer).

Reactions were performed in duplicate for each measurement, and substrate turnovers ranged between 14% and 20%. For Avi-GCPII, two separate measurements were performed. The K_m and k_{cat} values were determined from reaction rate versus substrate concentration plots using the GraFit program [35].

HPLC assay of carboxypeptidase activity

Kinetic constants of *N*-acetyl-L-aspartyl-L-methionine (Ac-Asp-Met) cleavage by Avi-GCPII and rhGCPII were determined using HPLC for quantification of the hydrolysis products. An appropriate amount of enzyme was added to reaction buffer (20 mM NaCl, 20 mM MOPS, pH 7.4) to final volume of 45 μL . The reaction mixtures were pre-incubated for 10 min at 37 °C. Then, 5 μL of substrate was added into each reaction (final concentration of substrate ranged from 2.8 μM to 360 μM). The reaction mixtures were incubated for 15 min at 37 °C and then stopped by adding 125 μL of ice-cold 0.2 M sodium borate, pH 10.0, and 4 μM L-glutamate (internal standard). Subsequently, the amount of free L-methionine was determined following a previously described method based on *o*-phthalaldehyde (OPA) derivatization [36] and analyzed on an Agilent 1200 Series system using an AccQ-Tag Ultra column (2.1 \times 100 mm; Waters).

Reactions were performed with substrate turnovers ranging from 10% to 15%. Methionine quantification was performed using a calibration curve constructed from known concentrations of methionine standard. The measurements were performed in duplicate for both proteins. The K_m and k_{cat} values were determined from reaction rate versus substrate concentration plots using the GraFit program [35].

Active site titration of Avi-GCPII and rhGCPII

Mixtures of an appropriate amount of enzyme (to achieve 10–15% substrate turnover for the non-inhibited reaction) and the tight-binding inhibitor 2-PMPA (final concentration ranging from 0 nM to 500 nM) in reaction buffer (20 mM NaCl, 20 mM MOPS, pH 7.4) were pre-incubated for 10 min at 37 °C. Reactions were started by addition of Ac-Asp-Met (final concentration 100 μM) and stopped after 15 min by addition of ice-cold 0.2 M sodium borate, pH 10.0, and 4 μM L-glutamate (internal standard). Reaction volumes and determination of free L-methionine were the same as for the carboxypeptidase activity assay.

The active site concentrations and K_i' values were determined from proportional velocity versus 2-PMPA concentration plots using the GraFit program [35].

Determination of the inhibition constant of 2-PMPA for Avi-GCPII and rhGCPII

The K_i for 2-PMPA was calculated from the K_i' value obtained during active site titration measurements following the formula: $K_i = K_i' / (1 + [S] / K_m)$ where [S] stands for Ac-Asp-Met concentration and K_m for the Michaelis constant of the enzyme towards Ac-Asp-Met.

Amino acid analysis

The total protein concentration of Avi-GCPII and rhGCPII stock solution was determined by analysis performed on a Biochrom30 amino acid analyzer (Biochrom) following the manufacturer's protocol.

Results

Preparation of the stable insect cell line expressing biotinylated Avi-GCPII

The DNA encoding AviTEV tag was prepared from oligonucleotides by the gene fusion approach and inserted into the plasmid pMNAEXST, which enables inducible expression in *Drosophila* Schneider 2 (S2) cells [19]. Cells stably transfected with this plasmid expressed rhGCPII N-terminally fused with AviTEV tag (Avi-GCPII) into the medium (the composition of the tag is schematically shown in Fig. 1, panel A). The cells were subsequently transfected with a plasmid encoding *E. coli* biotin-protein ligase (*BirA*). In order to analyze the efficiency of Avi-GCPII *in vivo* biotinylation, three different plasmids were prepared encoding *BirA* localized in cytoplasm (pMT/*BirA*), within the ER (pMT/*BiP*/*BirA*/KDEL), and secreted into the media (pMT/*BiP*/*BirA*). Two peptide signal sequences for *BirA* targeting were used: the *BiP* sequence for the secretory pathway and the KDEL sequence for retaining *BirA* within the ER.

The expression of Avi-GCPII in the cell lines stably transfected with *BirA* and Avi-GCPII was monitored by the Western blot (see Fig. 2). To determine the biotinylation efficiency, two visualizing agents were used: the monoclonal antibody GCP-04, which specifically recognizes the extracellular portion of GCPII (rhGCPII) [37], and NeutrAvidin conjugated with horseradish peroxidase (Neu-HRP), which visualizes only the biotinylated fraction of Avi-GCPII (and potential other endogenously biotinylated proteins). The cytoplasmic localization of *BirA* led to a very low biotinylation yield. On the other hand, the localization of *BirA* either within the ER or the secretory pathway caused the effective biotinylation of Avi-GCPII. Densitometry analysis of the Western blot revealed that *BirA* localization within the ER resulted in a slightly higher biotinylation yield compared to *BirA* localized in the secretory pathway (the ratio of the signals of biotinylated and total Avi-GCPII for *BirA* localized within the ER was approximately 15% higher than for *BirA* localized in secretory pathway). Based on these results, the cell line containing *BirA* within the ER (stable cell line 1) was used for large-scale expression of Avi-GCPII.

Previous work suggested that the addition of exogenous D-biotin into the cell medium might influence the *BirA* biotinylation efficiency [15]. However, this approach did not lead to any significant improvement in biotinylation efficiency in our hands (data not shown).

Avi-GCPII is successfully purified on Streptavidin Mutein Matrix

The purification protocol given by the manufacturer of Streptavidin Mutein Matrix (Roche) was changed for the purpose of Avi-GCPII purification. The appropriate amount of resin, buffer composition and its ionic strength, and incubation times were all optimized to provide the highest possible yield while sustaining high homogeneity of the purified protein.

After optimization of the purification protocol, large-scale purification of concentrated conditioned media was performed (see "Materials and methods" section for details). Fractions collected during purification were analyzed and their purity assessed by reducing SDS-PAGE (see Fig. 1, panel B for analysis of fractions

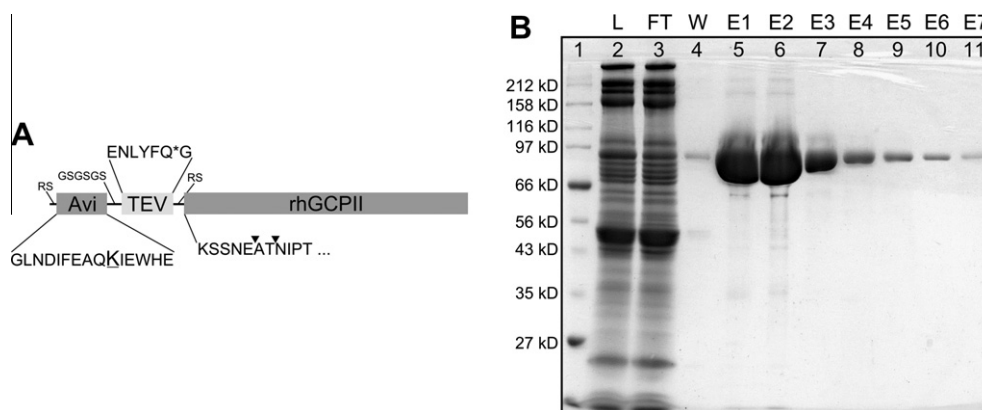


Fig. 1. Schematic representation of Avi-GCPII and analysis of its purification. *Panel A:* Schematic representation of Avi-GCPII with amino acid sequences detailed for all AviTEV tag parts; Avi – sequence of 15 amino acids known as AviTag, which is specifically recognized by biotin-protein ligase and biotinylated on the ε-amino group of the lysine residue (underlined); TEV – protein sequence specifically recognized by TEV protease (cleavage site is marked with *); rhGCPII – extracellular portion of GCPII consisting of amino acids 44–750. ▼ - identified cleavage site within Avi-GCPII recognized by an unknown host protease which is co-purified with Avi-GCPII. Spacer sequence and amino acids introduced during molecular cloning are depicted in a smaller font size. *Panel B:* Analysis of Avi-GCPII purification on Streptavidin Mutein Matrix. Equilibrated concentrated conditioned medium from S2 cells was mixed with resin and incubated overnight at 4 °C. The resin was separated from the medium on a gravity-flow column, and purified protein was eluted with an excess of D-biotin. Individual fractions obtained during purification were subsequently analyzed by SDS-PAGE and stained by Coomassie blue. (1). Molecular weight marker; (2). Load; (3). Flow-through; (4). Wash; (5–11). Elutions 1–7. Four microliters of the sample was loaded to each lane. Detailed descriptions of individual fractions can be found in “Materials and methods” section.

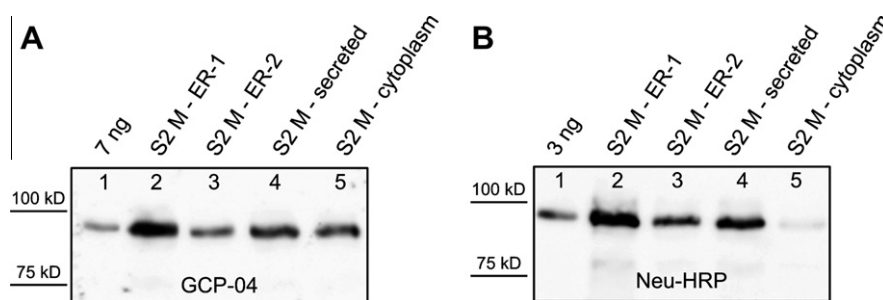


Fig. 2. Comparison of the biotinylation efficiency of *BirA* in different cellular compartments of S2 cells. Conditioned media from the cells, expressing Avi-GCPII and *BirA* (targeted to three different cellular compartments - cytoplasmic, secreted, or within the ER), were harvested 3 days post-induction and analyzed on Western blot. Western blots were visualized with the monoclonal antibody GCP-04, which recognizes total Avi-GCPII (panel A), and Neu-HRP, which recognizes only the biotinylated Avi-GCPII (panel B). (1) 7 ng (panel A) or 3 ng (panel B) of Avi-GCPII standard; (2) medium from cells with *BirA* localized within the ER (stable cell line 1); (3) medium from cells with *BirA* localized within the ER (stable cell line 2); (4) medium from cells with secreted *BirA*; (5) medium from cells with *BirA* localized in cytoplasm. Lanes 2–5 in both panels contained identical volumes of the analyzed samples.

from first purification). To increase the yield of purified Avi-GCPII, the affinity purification was performed in two rounds, with the flow-through from the first round used as an input for the second. The yields from the first and second round of purification were 4.3 mg and 0.7 mg of Avi-GCPII protein, respectively. The homogeneity of the purified protein was more than 95% and more than 90% of the protein was present in the first two elution fractions (E1, E2). The amount of Avi-GCPII in the cell conditioned medium before concentration and purification was estimated by densitometry analysis to be approximately 20 mg of overall and 12 mg of biotinylated Avi-GCPII in 0.8 L of the cell culture, suggesting that the purification yield was approximately 40%.

The purified Avi-GCPII was characterized and compared to its non-tagged version, the rhGCPII. We analyzed the influence of AviTEV tag on Avi-GCPII activity and crystallizability. We also investigated the possibility of removing the AviTEV tag with TEV protease.

The Avi-GCPII structure is not influenced by the attachment of the AviTEV tag

Purified Avi-GCPII was concentrated to 10 mg/mL and co-crystallized with a potent GCPII inhibitor, 2-(phosphonomethyl)-

pentanedioic acid (2-PMPA), using conditions identical to those used for rhGCPII crystallization [38]. The Avi-GCPII structure was obtained by the structural refinement of isomorphous structure of rhGCPII (PDB entry 2PVW) at 1.60 Å resolution, using the X-ray data collected for Avi-GCPII crystals. The new structure was deposited in the Protein Data Bank (PDB entry 3RBV). Detailed information about data collection and refinement statistics are summarized in Table 1.

The structure is virtually identical to that of rhGCPII (PDB entry 2PVW) with r.m.s.d. of 0.14 Å for 649 equivalent Cα atoms (see Fig. 3, panel A). In particular, residues participating in Zn²⁺ chelation and inhibitor binding retain their spatial arrangement (see Fig. 3, panels B and C). The AviTEV tag and the first 11 residues of rhGCPII are not visible in the electron density map, suggesting a high flexibility of the N-terminal part of the protein.

Avi-GCPII activity is not affected by the presence of the AviTEV tag

As a prerequisite for a careful quantitative comparison of Avi-GCPII and rhGCPII enzymatic activity, the total protein concentrations and the active site concentrations of both enzymes were determined by quantitative amino acid analysis and active site titration by a specific inhibitor. Relative portion of the

Table 1
Data collection and refinement statistics for the Avi-GCPII structure (3RBU).

Data collection statistics	
Wavelength (Å)	1.000
Temperature (K)	100
Space group	I222
Unit cell parameters <i>a</i> , <i>b</i> , <i>c</i> (Å)	101.3, 130.6, 158.9
Resolution limits (Å)	30.0–1.60 (1.66–1.60) ^a
Number of unique reflections	136,479 (12,595)
Redundancy	7.0 (4.4)
Completeness (%)	99.0 (91.9)
<i>I</i> /mean <i>I</i>	19.8 (2.4)
Rmerge	0.081 (0.517)
Refinement statistics	
Resolution limits (Å)	28.46–1.60 (1.64–1.60)
Total No. of reflections	134,416
No. of reflections in working	133,053 (8872)
No. of reflections in test set	1363 (68)
<i>R</i>	0.158 (0.251)
<i>R</i> _{free}	0.182 (0.255)
Total No. of non-H atoms	6770
No. of protein atoms	6050
No. of inhibitor atoms	14
No. of ions	4
No. of water molecules	702
Average B-factor (Å ²)	30.31
Protein atoms	28.32
Waters	42.11
Inhibitor	28.00
RMS deviations	
Bond lengths (Å)	0.018
Bond angles (deg)	1.689
Ramachandran plot (%)	
Favoured region	97.8%
Allowed region	2.05%
Disallowed region	0.15% (Gly335)
Missing residues	T1–T32, 44–54, 541–544, 655

The amino acids which belong to the AviTEV tag are denoted as Txy.

^a Values in parentheses correspond to the highest resolution shell.

enzymatically active molecules in the stock solution was assessed to be $102 \pm 2\%$ for Avi-GCPII and $72 \pm 2\%$ for the rhGCPII, respectively. The rhGCPII was purified according to the protocol established in our laboratory [19].

Kinetic constants characterizing cleavage of the prototypical GCPII substrate Ac-Asp-Glu [28], the less-efficient substrate Ac-Asp-Met [19], and the potent inhibitor 2-PMPA [39] were determined in order to characterize the effect of AviTEV tag on Avi-GCPII enzymatic activity. As shown in Table 2, all kinetic constants are comparable for both Avi-GCPII and rhGCPII, indicating that AviTEV tag does not affect the enzymatic characteristics of Avi-GCPII.

Avi-GCPII is ineffectively processed by TEV protease

The AviTEV tag was designed with the specific cleavage site for the tobacco etch virus (TEV) protease to enable the removal of the tag from Avi-GCPII (see Fig. 1, panel A). TEV protease is known as one of the most specific proteolytic enzymes and is widely used for the processing of recombinant proteins [40]. The purified, tagged TEV protease [His-TEV(S219V)-Arg] was incubated with purified Avi-GCPII in two different ratios (equimolar and with a 100-fold molar excess of TEV protease to Avi-GCPII). Cleavage was performed in three different buffers (see “Materials and methods” section). The results were identical for all buffers used, and for simplicity, only the experiment using TBS is shown in Fig. 4. It is visible from the Western blot analysis that a 100-fold molar excess of TEV protease is needed to efficiently remove the AviTEV tag, suggesting that the cleavage by TEV protease proceeds inefficiently, and its use in large-scale experiments would not be feasible.

Avi-GCPII is processed by host protease

Interestingly, a cleavage within the N-terminal part of purified Avi-GCPII itself was observed. N-terminal sequencing analysis identified two cleavage sites within the Avi-GCPII molecule (see Fig. 1, panel A). A series of experiments was performed in order to determine whether the processing is due to auto-proteolysis or hydrolysis by some host contaminating protease. The data shown in Fig. 5 suggested that Avi-GCPII is probably cleaved by a contaminant serine protease, since addition of a specific serine protease inhibitor, Pefabloc, slowed down the processing. The intensive degradation of Avi-GCPII observed in the experiment with EDTA was probably caused by chelation of zinc and calcium ions within Avi-GCPII and the protein's subsequent structural destabilization by which more cleavage sites became accessible for the contaminant host protease. This contaminant protease is probably not co-purified during the standard purification of rhGCPII since no N-terminal cleavage was observed for rhGCPII (data not shown).

Additional experiments showed that the cleavage is also effectively slowed at 4 °C and no hydrolysis of purified Avi-GCPII was detected after 2 days incubation at this temperature. To ensure the integrity of our protein preparation, the potential degradation of Avi-GCPII was examined under the conditions of enzymatic assays and protein crystal growth. In both these conditions no Avi-GCPII processing whatsoever was observed (data not shown).

Discussion

Simple, efficient, and robust recombinant protein expression and purification is indispensable for many areas of molecular biology, from structural genomics to protein–protein interaction studies. Even though expression and purification in prokaryotic expression systems is reasonably characterized, the eukaryotic systems still remain a challenge. We aimed to develop a well-functioning one-step purification procedure utilizing a biotin acceptor peptide (BAP) as a purification tag, for its well-characterized properties of binding to streptavidin and its analogs, and *Drosophila* S2 cells as an expression system, for their relatively easy handling, possibility of large-scale growth in suspension, and high expression yields. As a target protein, we chose glutamate carboxypeptidase II. Even though a purification protocol for this protein has already been developed [19], it is quite laborious and not much versatile. Even a single amino acid mutation influences the purification yield and requires some optimization [41] and for the GCPII homologs, however close, the method needs to be re-developed. [27]. We decided to locate the AviTEV tag on the N-terminus of rhGCPII since its 3D structure indicates that it is more flexible than C-terminus of the molecule.

This purification set-up requires preparation of stable cell line expressing both *E. coli* biotin-protein ligase (*BirA*) and the target recombinant protein. Previously published results describing the influence of *BirA* cellular localization (cytoplasmic, within the ER, or in the secretory pathway) on the biotinylation efficiency of secreted recombinant proteins fused with BAP were not complete. For instance, only two subcellular localizations were compared in parallel, and the results varied significantly between mammalian [10,11] and insect systems [15]. Therefore, we decided to prepare three stable insect cell lines with *BirA* localized in cytoplasm (*BirA*), within the ER (BiP-*BirA*-KDEL), or in secretory pathway (BiP-*BirA*), and compared them in terms of the biotinylation efficiencies of secreted Avi-GCPII.

The cytosolic localization of *BirA* was shown to be the least effective (see Fig. 2). This finding contradicts the results of Yang et al, who determined that cytosolic *BirA* had a higher biotinylation

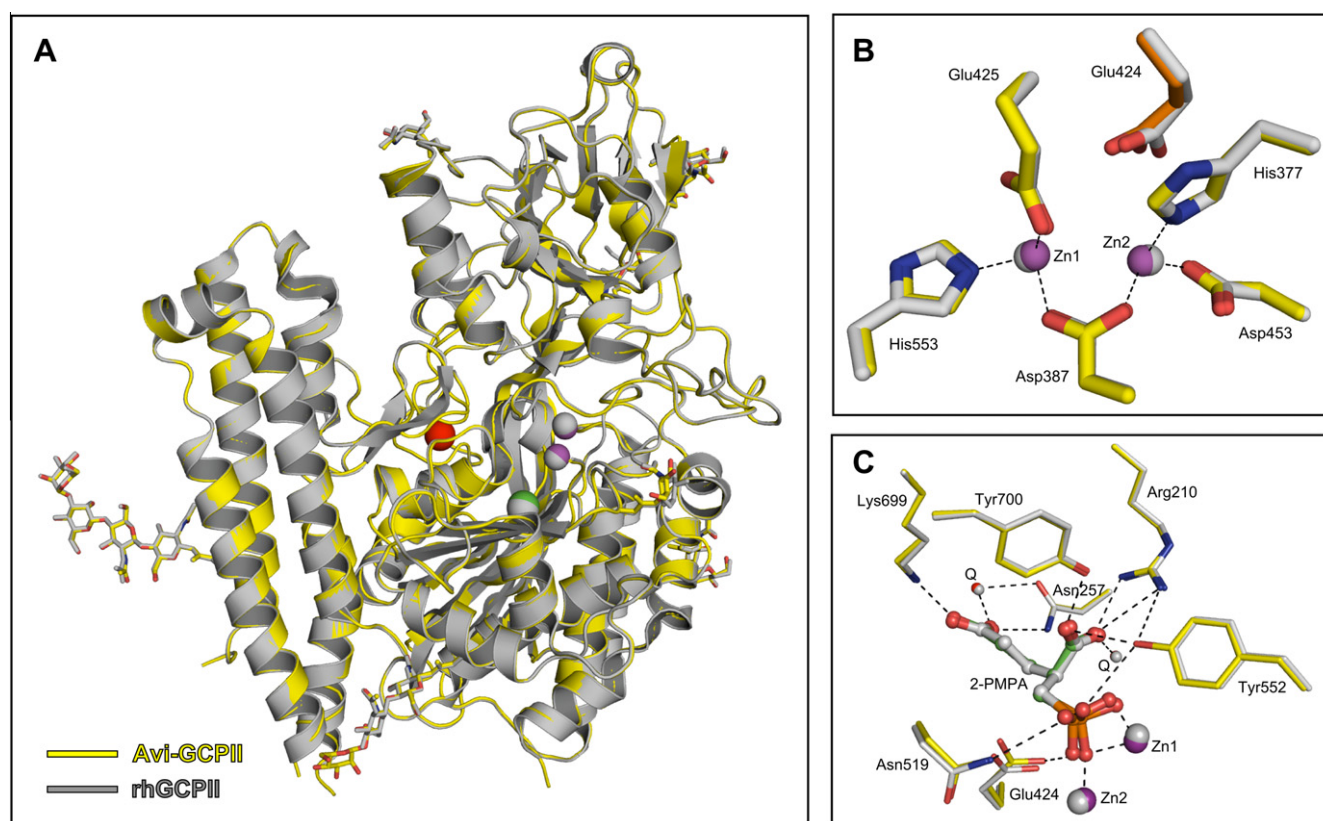


Fig. 3. Superposition of Avi-GCPII (3RBU) and rhGCPII (2PVW) structure. *Panel A:* The overall fold of Avi-GCPII and rhGCPII is identical. The protein backbone is shown in cartoon representation, sugar units in stick representation, and ions as spheres (Zn^{2+} – magenta, Cl^- – green, Ca^{2+} – red for Avi-GCPII). Avi-GCPII is shown in yellow, rhGCPII in gray (including ions and sugars). Sugar oxygens and nitrogens are shown in red and blue, respectively. *Panel B:* Superposition of the active site residues/atoms. Residues coordinating Zn^{2+} ions are shown in yellow and catalytic glutamate in orange for Avi-GCPII (Zn^{2+} ions as magenta spheres) while all rhGCPII residues are shown in gray (including ions). Oxygen atoms are depicted in red and nitrogen atoms in blue. Coordination of the active site zinc ions in the Avi-GCPII structure is shown as dashed lines. *Panel C:* 2-PMPA interactions in the Avi-GCPII/rhGCPII active sites. Avi-GCPII is shown in yellow (Zn^{2+} ions as magenta spheres, 2-PMPA in green ball-and-stick representation, waters Q as red spheres); rhGCPII in gray (including ions, 2-PMPA, and waters). Oxygen atoms are depicted in red, nitrogen atoms in blue, and the phosphorus atom in orange. Direct H-bonding and coordination to Zn^{2+} ions in the Avi-GCPII structure are shown as dashed lines. The figures were created using the PyMOL Molecular Graphics System [43].

Table 2
 Direct comparison of Avi-GCPII and rhGCPII enzymatic activity.

Substrate	Avi-GCPII			rhGCPII		
	K_m [$\mu\text{mol/L}$]	k_{cat} [per second]	k_{cat}/K_m [$10^5/s \cdot (\text{mol/L})$]	K_m [$\mu\text{mol/L}$]	k_{cat} [per second]	k_{cat}/K_m [$10^5/s \cdot (\text{mol/L})$]
Ac-Asp-Glu	0.53 ± 0.08^a	0.46 ± 0.01^a	8.66 ± 1.4	1.06 ± 0.18^a	0.41 ± 0.02^a	3.88 ± 1.06
Ac-Asp-Met	20.8 ± 3.3^b	0.29 ± 0.01^b	0.14 ± 0.02	25.2 ± 4.0^b	0.34 ± 0.02^b	0.13 ± 0.02
Inhibitor	K_i [pmol/L]			K_i [pmol/L]		
2-PMPA	370 ± 80^b			540 ± 120^b		

^a Measurements were performed by radioactive assay.

^b Measurements were performed by HPLC assay.

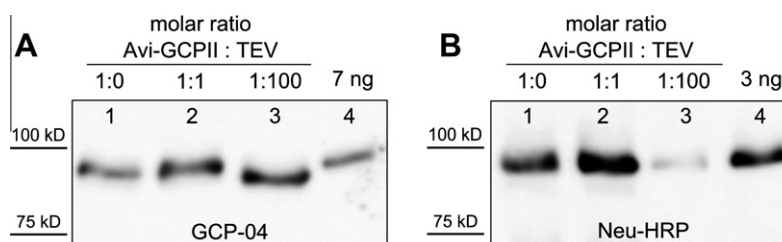


Fig. 4. Avi-GCPII cleavage by TEV protease. Purified Avi-GCPII was mixed with TEV protease in different ratios. The reactions were incubated overnight at 4 °C and then analyzed using Western blots. Blots were visualized with the monoclonal antibody GCP-04, which recognizes total Avi-GCPII (panel A), and Neu-HRP, which recognizes only biotinylated Avi-GCPII (panel B). (1) Purified Avi-GCPII without TEV protease; (2) equimolar mixture of Avi-GCPII and TEV protease; (3) Avi-GCPII with a 100-fold molar excess of TEV protease; 4. 7 ng (panel A) or 3 ng (panel B) of Avi-GCPII standard. Lanes 1–3 in both panels contained identical volumes of the analyzed samples.

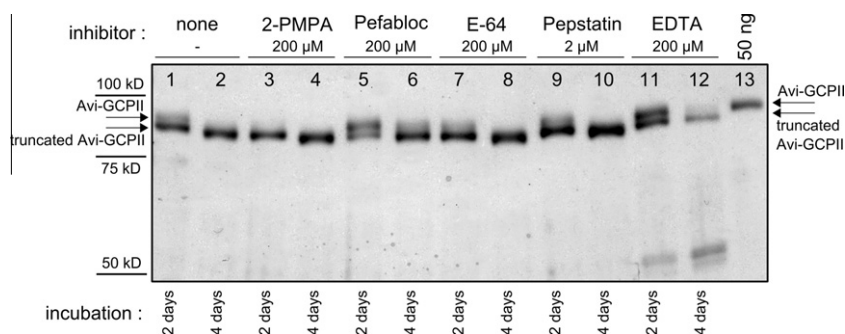


Fig. 5. Inhibition of Avi-GCPII cleavage by protease class-specific inhibitors. Purified Avi-GCPII was incubated at room temperature, and samples were taken after 2 days (lanes 1,3,5,7,9,11) and 4 days (lanes 2,4,6,8,10,12) and analyzed on silver-stained reducing SDS-PAGE. Inhibitors tested: 2-PMPA (specific GCPII inhibitor; final concentration 200 μ M; lanes 3,4), Pefabloc SC (serine protease inhibitor; final concentration 200 μ M; lanes 5,6), E-64 (cysteine protease inhibitor; final concentration 200 μ M; lanes 7,8), Pepstatin A (aspartate protease inhibitor; final concentration 2 μ M; lanes 9,10), EDTA (metalloprotease inhibitor; final concentration 200 μ M; lanes 11,12). The experiment without inhibitor was also performed (lanes 1, 2). Three microliters of the sample was loaded to each lane. 50 ng of purified Avi-GCPII was loaded to line 13 as a standard.

yield than the secreted form of *BirA* in insect cells [15]. This discrepancy might be due to the use of different peptide leading sequences for the secretion of *BirA* and target protein (BiP versus HLA-DR β leader sequence), by different localization of AviTag in the target molecule (N-terminal versus C-terminal), or by less obvious properties of a target protein or expression system. On the other hand, localizations of *BirA* within the ER and in the secretory pathway led to efficient Avi-GCPII biotinylation, indicating that the biotinylation in both cases probably proceeds within the ER. Only a slightly better relative biotinylation efficiency was determined for *BirA* localized within the ER compared to *BirA* localized in the secretory pathway. These data were consistent with the observations of Barat et al. in mammalian cells (even though we determined a much smaller difference between cells with secreted *BirA* and *BirA* retained within the ER) [11]. Additionally, it should be noted that using presented protocol for creation of stable S2 cell transfectants we obtained a polyclonal cell lines. When the transfection was done in duplicates, it showed higher variability in overall expression yields of biotinylated Avi-GCPII (Fig. 2, lanes 2 and 3) than was observed between cell lines with differently localized *BirA* (Fig. 2, lanes 2 and 4). These findings suggest that the careful optimization of the expression system is at least as important as proper localization of biotin ligase within the cell.

The purification procedure itself was optimized to provide the highest possible yield while preserving high homogeneity of the purified protein. Surprisingly, the use of non-dialyzed conditioned medium as a starting material for purification was shown to be the best option. Dialysis of the medium followed by optimization of ionic strength and/or addition of exogenous D-biotin resulted in lower yields and/or purity (data not shown). This effect might have been caused by some unknown additive present in the SF900II medium. We have also observed that by concentrating the conditioned medium prior to affinity purification, we improved greatly the purification yield. The explanation of this observation is not straightforward: it might be caused by increasing the effective concentration of both Avi-GCPII and mitein resin beads within the incubation mixture. Similar behavior was also observed during purifications of several Avi-GCPII mutants and homologs (data not shown).

Tags covalently attached to purified protein are useful tools for subsequent visualization or immobilization and are often retained with the target protein. In the case of AviTEV tag, the covalently attached biotin enables easy visualization, immobilization, or specific uptake of the target protein. Since the AviTEV tag is not effectively cleaved from its fusion partner by TEV protease, we focused on a detailed analysis of its influence on the biochemical features of rhGCPII.

We were able to crystallize Avi-GCPII under conditions identical to those used for the non-tagged enzyme, suggesting that the AviTEV tag does not influence the ability of Avi-GCPII to crystallize. In fact, we showed that the structure of Avi-GCPII is virtually identical to that of rhGCPII. A lack of interpretable electron density for the AviTEV tag indicates that this motif is likely disordered. Furthermore, we solved a structure of the AviTEV-tagged extracellular part of Naaladase L (amino acids 28–740), a GCPII homolog, in which the AviTEV tag was also not visible (manuscript in preparation). Those findings, together with a previously reported study of the structure of maltodextrin-binding protein fused with biotin acceptor peptide [42], supports the conclusion that the presence of AviTEV tag does not significantly affect the 3D structure of its fusion partner.

To determine the effect of AviTEV tag on Avi-GCPII enzymatic activity, kinetic constants for cleavage of GCPII substrates Ac-Asp-Glu and Ac-Asp-Met and the inhibition constant for the potent GCPII inhibitor 2-PMPA were determined for both Avi-GCPII and rhGCPII (see Table 2). The slightly improved catalytic efficiency of Avi-GCPII compared to rhGCPII might be explained by the milder conditions of the purification procedure used for Avi-GCPII. This notion was also supported by active site titration measurements. Purification via AviTEV tag led to Avi-GCPII molecules that were nearly 100% enzymatically active, while the standard four-step purification method yielded only 72% enzymatically active rhGCPII. The lower relative representation of enzymatically active enzyme in rhGCPII preparation compared to Avi-GCPII may be caused by complexity of purification (4 steps versus 1 step) and overall duration of purification procedure (approximately 5 days versus 2 days) in the former case. The inactive fraction of rhGCPII might partially bind the substrate/inhibitor and thus lower the observed catalytic efficiency of rhGCPII. The k_{cat} values for rhGCPII presented in Table 2 are not quite in agreement with previously published data [19,27]. This discrepancy might be caused by different methods of protein concentration determination (active site titration versus Bradford assay). Taken together, we can conclude that in this purification set-up AviTEV tag does not compromise the enzymatic activity of its fusion partner.

Even though the N-terminus part of Avi-GCPII molecule is disordered and accessible for host contaminant protease, the TEV protease showed to be very inefficient in cleaving off the tag. The poor processing may be caused by the arginine residue located at the P2' position of the TEV cleavage site in Avi-GCPII molecule (see Fig. 1, panel A). In support of this hypothesis, we checked the enzymatic activity of the same preparation of TEV protease and determined it successfully cleaved different fusion protein containing TEV cleavage site (data not shown).

A potential versatility of this purification set-up was confirmed by successful purification of Avi-GCPII site-directed mutants and also several of its human paralogs and animal orthologs (data not shown). Furthermore, a secreted version of a different enzyme, carbonic anhydrase IX, with the AviTEV tag on its C-terminus was also successfully expressed and purified (Mader et al., manuscript in preparation). It might be relevant to mention that carbonic anhydrase XI is a type I transmembrane protein, and, consequently, the topology of the AviTEV tag location was the same as for Avi-GCPII)

In conclusion, we prepared a cell line of stably transfected *Drosophila* S2 cells with *BirA* localized within the ER and compared it with stable cell lines with the cytosolic and secreted forms of *BirA*. We showed that *BirA* localizations within both the ER and the secretory pathway lead to efficient biotinylation of target protein while the localization within ER showed slightly better biotinylation yield. Using this stable cell line we expressed, purified and characterized recombinant human GCPII. We achieved milligrams yields of pure protein per liter of culture and showed that AviTEV tag does not compromise the features of its fusion partner. Since the interaction is independent of target protein properties, we believe this purification set-up may represent a versatile and facile method for efficient expression and purification of secreted recombinant proteins in *Drosophila* S2 cells.

Acknowledgments

The authors thank Karolína Šrámková for excellent technical assistance, Klára Hloučová for preparation of rhGCPII protein, Zdeněk Voburka for N-terminal sequencing analysis, Martin Hradíček for synthesis of tested *N*-acetylated dipeptides, Radko Souček for expert HPLC analysis, and Hillary Hoffman for preparation of TEV protease and insightful proofreading of the manuscript. The plasmid encoding TEV protease was a kind gift from David Waugh (National Cancer Institute at Frederick, NIH, MD, USA), and the inhibitor 2-PMPA was a kind gift from Barbara Slusher (School of Medicine, Johns Hopkins University, MD, USA).

This work (performed under the research project Z4 055 905) was supported by Grants 1M0508 and LC 512 from the Ministry of Education of Czech Republic, EMBO Installation Grant #1978 (C.B), the IBT institutional support (AV0Z50520701), by research support from Guilford Pharmaceuticals, and in part by the Intramural Research Program of the NIH, National Cancer Institute, Center for Cancer Research (J.L.). Use of the Advanced Photon Source was supported by the US Department of Energy, Office of Science, Office of Basic Energy Sciences, under Contract No. W-31-109-Eng38.

References

- [1] N.M. Green, Avidin. 1. The use of (14-C)biotin for kinetic studies and for assay, *Biochem. J.* 89 (1963) 585–591.
- [2] M.H. Qureshi, S.L. Wong, Design, production, and characterization of a monomeric streptavidin and its application for affinity purification of biotinylated proteins, *Protein Expr. Purif.* 25 (2002) 409–415.
- [3] S.C. Wu, S.L. Wong, Engineering soluble monomeric streptavidin with reversible biotin binding capability, *J. Biol. Chem.* 280 (2005) 23225–23231.
- [4] M.D. Lane, K.L. Rominger, D.L. Young, F. Lynen, The enzymatic synthesis of holotranscarboxylase from apotranscarboxylase and (+)-biotin. II. Investigation of the reaction mechanism, *J. Biol. Chem.* 239 (1964) 2865–2871.
- [5] M.D. Lane, D.L. Young, F. Lynen, The enzymatic synthesis of holotranscarboxylase from apotranscarboxylase and (+)-biotin. Purification of the apoenzyme and synthetase; characteristics of the reaction, *J. Biol. Chem.* 239 (1964) 2858–2864.
- [6] D. Beckett, E. Kovaleva, P.J. Schatz, A minimal peptide substrate in biotin holoenzyme synthetase-catalyzed biotinylation, *Protein Sci.* 8 (1999) 921–929.
- [7] P.J. Schatz, Use of peptide libraries to map the substrate specificity of a peptide-modifying enzyme: a 13 residue consensus peptide specifies biotinylation in *Escherichia coli*, *Biotechnology (NY)* 11 (1993) 1138–1143.
- [8] E. de Boer, P. Rodriguez, E. Bonte, J. Krijgsveld, E. Katsantoni, A. Heck, F. Grosveld, J. Strouboulis, Efficient biotinylation and single-step purification of tagged transcription factors in mammalian cells and transgenic mice, *Proc. Natl. Acad. Sci. USA* 100 (2003) 7480–7485.
- [9] S. Duffy, K.L. Tsao, D.S. Waugh, Site-specific, enzymatic biotinylation of recombinant proteins in *Spodoptera frugiperda* cells using biotin acceptor peptides, *Anal. Biochem.* 262 (1998) 122–128.
- [10] A. Predonzani, F. Arnoldi, A. Lopez-Requena, O.R. Burrone, In vivo site-specific biotinylation of proteins within the secretory pathway using a single vector system, *BMC Biotechnol.* 8 (2008) 41.
- [11] B. Barat, A.M. Wu, Metabolic biotinylation of recombinant antibody by biotin ligase retained in the endoplasmic reticulum, *Biomol. Eng.* 24 (2007) 283–291.
- [12] S. Driegen, R. Ferreira, A. van Zon, J. Strouboulis, M. Jaegle, F. Grosveld, S. Philipsen, D. Meijer, A generic tool for biotinylation of tagged proteins in transgenic mice, *Transgenic Res.* 14 (2005) 477–482.
- [13] K. Sung, M.T. Maloney, J. Yang, C. Wu, A novel method for producing mono-biotinylation, biologically active neurotrophic factors: an essential reagent for single molecule study of axonal transport, *J. Neurosci. Methods* 200 (2011) 121–128.
- [14] D. Juzumiene, C.Y. Chang, D. Fan, T. Hartney, J.D. Norris, D.P. McDonnell, Single-step purification of full-length human androgen receptor, *Nucl. Recept. Signal.* 3 (2005) e001.
- [15] J. Yang, A. Jaramillo, R. Shi, W.W. Kwok, T. Mohanakumar, In vivo biotinylation of the major histocompatibility complex (MHC) class II/peptide complex by coexpression of *BirA* enzyme for the generation of MHC class II/tetramers, *Hum. Immunol.* 65 (2004) 692–699.
- [16] T.G. Schmidt, A. Skerra, The Strep-tag system for one-step purification and high-affinity detection or capturing of proteins, *Nat. Protoc.* 2 (2007) 1528–1535.
- [17] A. Skerra, T.G. Schmidt, Applications of a peptide ligand for streptavidin: the Strep-tag, *Biomol. Eng.* 16 (1999) 79–86.
- [18] J.J. Lichty, J.L. Malecki, H.D. Agnew, D.J. Michelson-Horowitz, S. Tan, Comparison of affinity tags for protein purification, *Protein Expr. Purif.* 41 (2005) 98–105.
- [19] C. Barinka, M. Rinnova, P. Sacha, C. Rojas, P. Majer, B.S. Slusher, J. Konvalinka, Substrate specificity, inhibition and enzymological analysis of recombinant human glutamate carboxypeptidase II, *J. Neurochem.* 80 (2002) 477–487.
- [20] C. Barinka, P. Sacha, J. Sklenar, P. Man, K. Bezouska, B.S. Slusher, J. Konvalinka, Identification of the N-glycosylation sites on glutamate carboxypeptidase II necessary for proteolytic activity, *Protein Sci.* 13 (2004) 1627–1635.
- [21] P. Buhler, P. Wolf, U. Elsasser-Beile, Targeting the prostate-specific membrane antigen for prostate cancer therapy, *Immunotherapy* 1 (2009) 471–481.
- [22] A.A. Elgamal, E.H. Holmes, S.L. Su, W.T. Tino, S.J. Simmons, M. Peterson, T.G. Greene, A.L. Boynton, G.P. Murphy, Prostate-specific membrane antigen (PSMA): current benefits and future value, *Semin. Surg. Oncol.* 18 (2000) 10–16.
- [23] A. Ghosh, W.D. Heston, Tumor target prostate specific membrane antigen (PSMA) and its regulation in prostate cancer, *J. Cell. Biochem.* 91 (2004) 528–539.
- [24] J.H. Neale, R.T. Olszewski, L.M. Gehl, B. Wroblewska, T. Bzdega, The neurotransmitter *N*-acetylaspartylglutamate in models of pain, ALS, diabetic neuropathy, CNS injury and schizophrenia, *Trends Pharmacol. Sci.* 26 (2005) 477–484.
- [25] R.E. Conway, N. Petrovic, Z. Li, W. Heston, D. Wu, L.H. Shapiro, Prostate-specific membrane antigen regulates angiogenesis by modulating integrin signal transduction, *Mol. Cell. Biol.* 26 (2006) 5310–5324.
- [26] T. Liu, M. Jabbes, J.R. Nedrow-Byers, L.Y. Wu, J.N. Bryan, C.E. Berkman, Detection of prostate-specific membrane antigen on HUVECs in response to breast tumor-conditioned medium, *Int. J. Oncol.* 38 (2011) 1349–1355.
- [27] K. Hloučová, C. Barinka, V. Klusak, P. Sacha, P. Mlcochova, P. Majer, L. Rulisek, J. Konvalinka, Biochemical characterization of human glutamate carboxypeptidase III, *J. Neurochem.* 101 (2007) 682–696.
- [28] M.B. Robinson, R.D. Blakely, R. Couto, J.T. Coyle, Hydrolysis of the brain dipeptide *N*-acetyl-L-aspartyl-L-glutamate. Identification and characterization of a novel *N*-acetylated alpha-linked acidic dipeptidase activity from rat brain, *J. Biol. Chem.* 262 (1987) 14498–14506.
- [29] W.S. Rasband, ImageJ. US National Institutes of Health, Bethesda, Maryland, USA. <http://www.rsby.info.nih.gov/ij/>, 1997–2008.
- [30] Z. Otwinowski, W. Minor, Processing of X-ray diffraction data collected in oscillation mode, *Methods Enzymol.* 276 (1997) 307–326.
- [31] C. Barinka, M. Rovenska, P. Mlcochova, K. Hloučová, A. Plechanovova, P. Majer, T. Tsukamoto, B.S. Slusher, J. Konvalinka, J. Lubkowski, Structural insight into the pharmacophore pocket of human glutamate carboxypeptidase II, *J. Med. Chem.* 50 (2007) 3267–3273.
- [32] G.N. Murshudov, A.A. Vagin, E.J. Dodson, Refinement of macromolecular structures by the maximum-likelihood method, *Acta Crystallogr. D Biol. Crystallogr.* 53 (1997) 240–255.
- [33] P. Emsley, K. Cowtan, Coot: model-building tools for molecular graphics, *Acta Crystallogr. D Biol. Crystallogr.* 60 (2004) 2126–2132.
- [34] V.B. Chen, W.B. Arendall 3rd, J.J. Headd, D.A. Keedy, R.M. Immormino, G.J. Kapral, L.W. Murray, J.S. Richardson, D.C. Richardson, MolProbity: all-atom structure validation for macromolecular crystallography, *Acta Crystallogr. D Biol. Crystallogr.* 66 (2010) 12–21.
- [35] R.J. Leatherbarrow, GraFit Version 5, Erithacus Software Limited, Horley, UK, 2001.
- [36] C. Woodward, J.K. Henderson, T. Wielgos, High-speed amino acid analysis (AAA) on 1.8 μm reversed-phase (RP) columns. Agilent Technologies App. Note (2007) 5989-6297EN.

- [37] P. Sacha, J. Zamecnik, C. Barinka, K. Hlouchova, A. Vicha, P. Mlcochova, I. Hilgert, T. Eckschlager, J. Konvalinka, Expression of glutamate carboxypeptidase II in human brain, *Neuroscience* 144 (2007) 1361–1372.
- [38] C. Barinka, J. Starkova, J. Konvalinka, J. Lubkowski, A high-resolution structure of ligand-free human glutamate carboxypeptidase II, *Acta Crystallogr., Sect. F: Struct. Biol. Cryst. Commun.* 63 (2007) 150–153.
- [39] P.F. Jackson, D.C. Cole, B.S. Slusher, S.L. Stetz, L.E. Ross, B.A. Donzanti, D.A. Trainor, Design, synthesis, and biological activity of a potent inhibitor of the neuropeptidase N-acetylated alpha-linked acidic dipeptidase, *J. Med. Chem.* 39 (1996) 619–622.
- [40] J. Phan, A. Zdanov, A.G. Evdokimov, J.E. Tropea, H.K. Peters 3rd, R.B. Kapust, M. Li, A. Wlodawer, D.S. Waugh, Structural basis for the substrate specificity of tobacco etch virus protease, *J. Biol. Chem.* 277 (2002) 50564–50572.
- [41] P. Mlcochova, A. Plechanovova, C. Barinka, D. Mahadevan, J.W. Saldanha, L. Rulisek, J. Konvalinka, Mapping of the active site of glutamate carboxypeptidase II by site-directed mutagenesis, *FEBS J.* 274 (2007) 4731–4741.
- [42] M.H. Bucher, A.G. Evdokimov, D.S. Waugh, Differential effects of short affinity tags on the crystallization of *Pyrococcus furiosus* maltodextrin-binding protein, *Acta Crystallogr. D Biol. Crystallogr.* 58 (2002) 392–397.
- [43] Schrodinger, LLC, The PyMOL Molecular Graphics System, Version 1.3r1, 2010.